CORROSION PROTECTION OF MRI230D MAGNESIUM ALLOY BY THE PLASMA ELECTROLYTIC OXIDATION

Barbara Kazanski Traubin, Alex Lugovskoy*, Michael Zinigrad

Department of Chemical Engineering, Ariel University, Ariel 70400, Israel

*Corresponding author: Alex Lugovskoy, e-mail lugovsa@ariel.ac.il

ABSTRACT

PURPOSE: The applicability of Plasma Electrolytic Oxidation for the corrosion of magnesium alloys in NaCl solutions was studied.

Design/methodology/approach: Oxide layers, whose thickness was ~20 μm, were produced by the Plasma Electrolytic Oxidation (PEO). Specimens of MRI230D alloy as cast and of the alloy treated by the PEO were immersed into the water solution of 3% NaCl. The corrosion process was monitored by (a) gas evolution, (b) mass loss, (c) Open Circuit Potential, (d) Electrochemical Impedance Spectroscopy, (e) Linear Polarization Resistance and (f) Tafel Slope Extrapolation. Corrosion rates for each method were calculated and compared.

Findings: The corrosion is localized so that corrosion pits are developed on a specimen surface. Corrosion rates measured by different methods are all on the order of magnitude of 0.25 – 3.7 mm / year. The protection of the alloy by the PEO decreases the rate of corrosion and shifts the corrosion potential to a more noble value.

Research limitations/implications: The localized character of corrosion causes significant deviations in the results obtained even by the same method; large deviations of corrosion rates are observed for all the methods.

Originality/value: To the best of our knowledge, this is the first study of the corrosion protection of die cast creep-resistant magnesium alloy MRI230D by the PEO.

Keywords: magnesium alloys; corrosion; plasma electrolytic oxidation; micro arc oxidation

INTRODUCTION

Light, strong, readily castable, weldable and recyclable magnesium alloys are becoming more and more popular for various branches of industries. However, their high vulnerability to corrosion presents a serious limitation to many applications. Among various ways to provide better protection of magnesium alloys from corrosion Plasma Electrolytic Oxidation (PEO) attracts growing attention both in science and industry. PEO treatment of magnesium alloy (Lugovskoy and Zinigrad, 2013) can produce a thick (tens to hundreds of microns), dense and hard oxide layer providing excellent protection from corrosion and wear.

MRI230D alloy belongs to the advanced materials developed to address the applications of the automotive industry such as engine blocks operating at temperatures up to 190°C. The alloy has excellent creep resistance combined with good castability, high strength and superior corrosion behavior. [1] The alloy contains 6.5% Al, 2% Ca, 0.8% Sn, 0.3% Mn and the balance of Mg.

The purpose of this paper is to find out, whether the corrosion behavior of MRI230D can be even more improved by its treatment by PEO. Several electrochemical and non-electrochemical techniques are applied for the determination of corrosion parameters.

EXPERIMENTAL

The electrolyte for the PEO contained 0.05 mol / L Na_2SiO_3 (pentahydrate, Spectrum, practical grade, silicate index n = 1), 0.04 mol / L KOH (Finkelman Chemicals, technical grade) and 0 – 0.2 mol / L KF (Merck, 99%) in tap water. All the procedures were performed at room temperature with only passive cooling by a 50 L water tank, in which the 3L PEO cell was set. The maximal heating in the course of the oxidation was 2-3°C and no influence of these temperature changes was observed. The oxidation was performed in AC mode by 50 Hz sew edged voltage at the average current density of approximately 10.0 ± 2.0 A / dm^2 on a purpose made 40 kVA PEO station with a water-cooled bath made of stainless steel, which served as the counter electrode. Each specimen (rectangular plates 20 X 30 X 3 mm) was oxidized for 30 minutes so that the initial and final voltages were 50V and 232-248V, respectively. The thickness of the produced oxide layer was 22-26 μm.

The corrosion was measured in 3 wt% NaCl solution at room temperature (20 ± 3°C). Rectangular plates of the alloy were polished, degreased with acetone, dried by air and packed into a polymer so that only 1.1 cm^2 area was exposed to the corrosion medium. Thus prepared specimens were left in a standard three-electrode cell (Ag|AgCl in sat. KCl solution was used as the reference electrode and a Pt wire served as the counter electrode) until a steady state corrosion potential was achieved. After the achievement of a stable corrosion potential (typically, 5-7 days) electrochemical measurements were performed with an Autolab PGStat12 potentiostat equipped with a FRA module for measuring the impedance.

Mass loss was measured after the immersion of a specimen into 3% NaCl solution for 11-20 days. After that the corrosion products were removed from the specimen by the solution of 200 g/L CrO_3 and 10 g/L $AgNO_3$ (Shi Z. and Atrens A., 2011; Arrabal *et al.*, 2012) until no bubbles evolved (5-10 min of immersion). After the removal of the corrosion products the specimens were washed with deionized water, dried with high pressure dry air and kept for 4 days in a vacuum desiccator.

For microstructural analysis, a scanning electron microscope (SEM, JEOL JSM-6510LV) and electron dispersive spectroscopy (EDS, Thermo scientific NS7) were used. For the SEM and EDS analysis a specimen was etched for about 2 sec in 2% nital solution (Qiao *et al*, 2012; Song *et al.*, 1999), washed with acetone and dried by pressured dry air.

Results

Both oxidized and not oxidized samples achieve steady potentials of, respectively, – 1.452 ± 0.004 V and – 1.474 ± 0.011 V vs. Ag|AgCl after 3-7 days (Figure 1). The average size of the visual pits is 0.5-1 mm both for the 'raw' and for the PEO treated alloy (Figure 2).

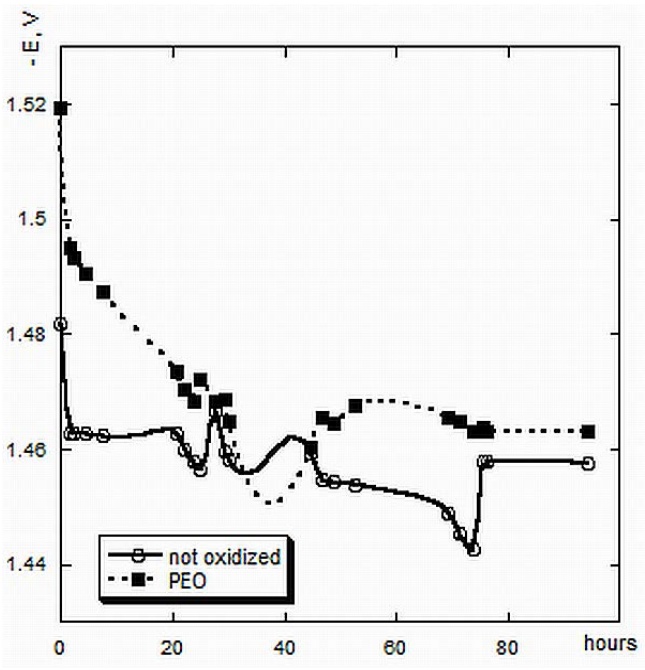

Figure 1. Stabilization of the corrosion potential (vs. Ag|AgCl) of MRI230D in 3% NaCl.

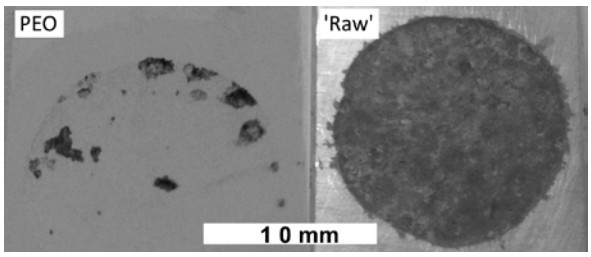

Figure 2. The surfaces of a 'raw' not oxidized sample (right) and of a PEO treated sample (left) after some days of immersion into 3% NaCl. Only the round window was open for the corrosion process, the rest of the surface sealed by a polymer.

The Electrochemical Impedance spectra (Figure 3) both of oxidized and not oxidized samples show a complex behavior. An inductive loop is present in all the impedance spectra, which can be explained as sorption of some ions on the metal surface. Two capacitive loops indicate that the electrochemical processes occur both at the metal-oxide interphase and inside the oxide layer.

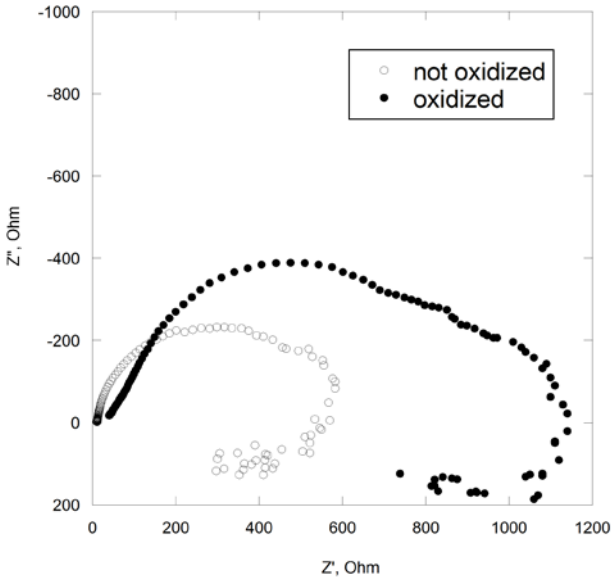

Figure 3. Typical EIS Nyquist plots for MRI230D in 3% NaCl.

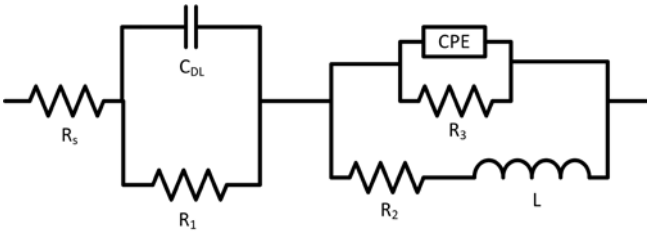

Figure 4. An equivalent circuit best fit to the measured EIS spectra.

Tafel slopes, corrosion potential and corrosion current were determined from the polarization curves measured in the potential range of - 0.250 V to +0.150V *vs.* the stable corrosion potential (Figure 5).

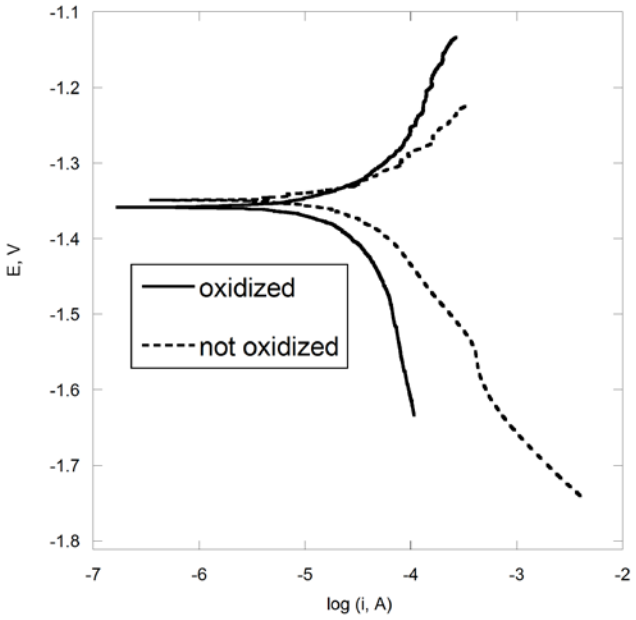

Figure 5. Tafel polarization plots for the PEO oxidized and not oxidized samples of MRI230D alloy.

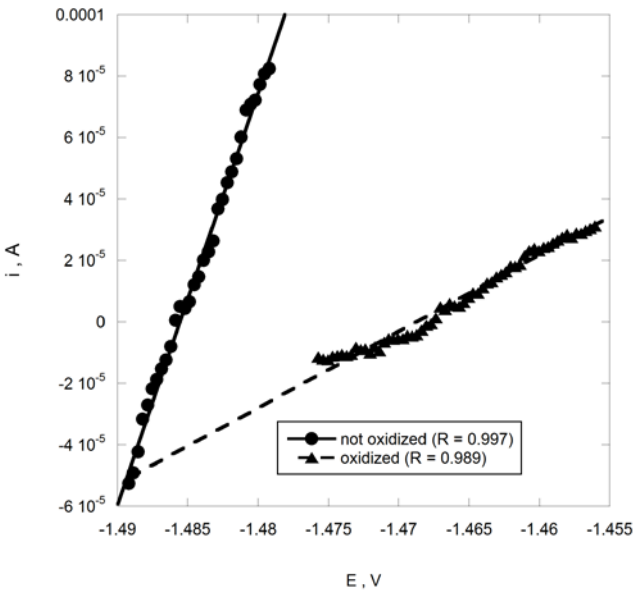

Figure 6. LPR plots for the PEO oxidized and not oxidized samples of MRI230D alloy.

Linear polarization resistance was calculated from the slope of the linear regression line to the polarization curve measured in the range of ± 10 mV *vs.* the corrosion potential. As is seen from Figure 6, the deviations of the polarization curve from the linear regression line are negligible in this range (R = 0.997 for the not oxidized sample and R = 0.989 for the oxidized sample).

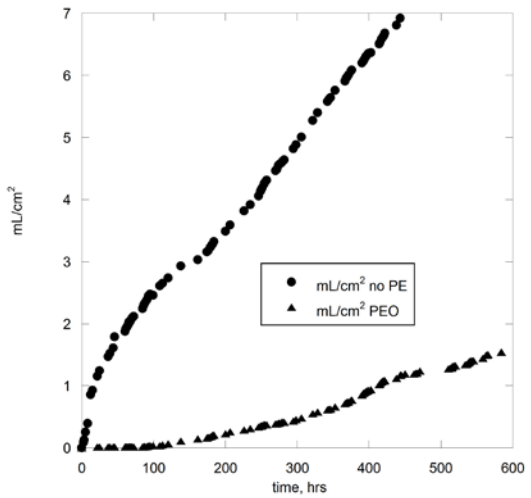

Figure 7. Plots of the gas evolution rate for the oxidized and not oxidized samples of MRI230D alloy.

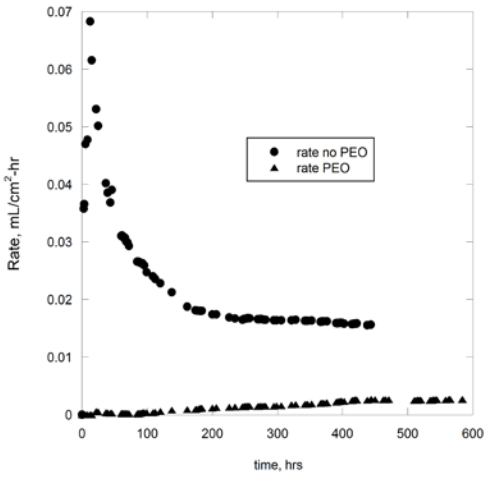

Figure 8. The time dependencies of the gas evolution rates for the oxidized and not oxidized samples of MRI230D alloy.

The corrosion rate calculated from the measurements of the gas evolution for an oxidized sample is much lower than that for a not oxidized sample (Figure 7). Moreover, while the time dependence of the rate for an oxidized sample is linear with a slight positive slope (Figure 8), the alloy not treated by the PEO demonstrates a pronounced exponential decay of the corrosion rate. The rates of corrosion measured by different methods are summarized in Table 1.

	R_{EIS}	R_{Tafel}	R_{LPR}	R_{gas}	$R_{mass\ loss}$
'raw' alloy	2.9	2.6	3.7	0.31	0.25
PEO treated	2.28	0.9	1.9	0.13	0.09

Table 1: Corrosion rates in mm/year for the 'raw' and PEO treated MRI230D alloy measured by different methods.

DISCUSSION

As is seen from Figure 1, for a 'raw' (not oxidized) sample already after a few first hours the potential is close to the steady value. Unlike that, much steeper potential change is observed for an oxidized sample, so that only on the second day of the immersion the potential approaches the steady state. For both kinds of samples significant “wells” of the potential are observed. Each “well” starts from the formation of a new corrosion pit (the potential becomes less negative) and ends a few hours later with the “healing” of it (the potential returns to the more negative value). The number of pits and the time of appearance of each pit are absolutely random, but the lifetime of a pit is quite constant: 3-5 hours for the not oxidized alloy and 8-10 hours for the oxidized samples.

Impedance spectra very similar to those shown in Figure 3 were observed by Chen *et al.* (Chen *et al.*, 2007) for AZ91D alloy in aqueous sodium sulfate. The spectra of both oxidized and not oxidized samples are best fit by the equivalent scheme shown in Figure 4. This equivalent circuit is identical to the circuit proposed by Chen *et al.* for the first hour of immersion and explained as “a charge transfer resistance R_1, in parallel with the double layer capacity C_{DL}, film resistance R_2 ($Mg(OH)_2$–$MgAl_2(OH)_8 \cdot H_2O$ film resistance), in parallel with CPE, and the inductance L induced by metastable Mg^+ ions in series with a charge transfer resistance R_3.” (*ibidem*) In spite the fact that the existence of Mg^+ remains questionable, this explanation is quite convincing and we accept it for our system, too. The corresponding fit parameters are given in Table 2.

	R_s, Ω	**R_1, Ω**	**C_{DL}, F**	**R_2, Ω**	**R_3, Ω**	**L, H**	**C_{CPE}, F**	**n_{CPE}**
Not oxidized	10.8	289.44	$6.01 \cdot 10^{-5}$	274.57	111.03	112.28	$2.23 \cdot 10^{-4}$	0.808
Oxidized	23.1	565.09	$5.44 \cdot 10^{-6}$	972.41	244.02	184.50	$3.52 \cdot 10^{-4}$	0.441

Table 2: Typical fit parameters of the measured EIS to the equivalent scheme shown in Figure 4

While the cathodic branch of a polarization curve (Figure 5) for the PEO treated sample has the characteristic Tafel shape, a break at the potential of about – 1.55V is observed for the cathodic branch of the sample without the oxidation. We could assume that some retardation of water reduction occurs at the potentials more negative than – 1.55V, but the detailed study of this issue is far beyond the scope of this paper.

The anodic branches of the Tafel plot are monotonous and show no passivation or other phenomena in the above potential range. However, attempts to increase the anodic polarization limit above +0.150V *vs.* E_{corr} immediately resulted in intense pitting and fast degradation of the specimen. The Tafel slopes are b_a = 172 mV/dec and b_c = 234 mV/dec for the not oxidized sample and b_a = 213 mV/dec and b_c = 506 mV/dec for the PEO treated one and the corrosion currents are $1.31 \cdot 10^{-4}$ A/cm^2 and $4.5 \cdot 10^{-5}$ A/cm^2, correspondingly.

Tafel slopes determined from the polarization curves (Figure 5) were used for the calculation of the Stern-Geary constant and its value for the not oxidized alloy was B = 43.1 mV / dec. For the alloy treated by PEO the value of the Stern-Geary constant was 65.2 mV / dec. The corrosion

current densities calculated from the LPR plots (Figure 6) are $1.85 \cdot 10^{-4}$ A/cm^2 for the not oxidized and $9.58 \cdot 10^{-5}$ A/cm^2 for the oxidized sample.

As is seen from Table 1, five methods provide five completely different sets of corrosion rates, the only common feature of which is the fact that the corrosion of a PEO treated sample is always slower than that of a 'raw' alloy specimen. Such a sorrowful situation is quite common for magnesium alloys (see, for example Atrens *et al.*, 2013). For our specific case, we can assume some explanations to these differences:

1. Both the EIS spectra and the equivalent circuit used here (Figures 3, 4) demonstrate quite clearly that the corrosion process has a very complex mechanism including sorption, diffusion and two charge-transfer steps. The calculation of the corrosion rates is based on the assumption that they are controlled by the charge-transfer resistance R_1. Obviously, the reality is less simple and a mixed control takes place.

2. Too high, especially for the PEO treated alloy, cathodic Tafel slopes hint that the diffusion of the Red species (presumably, water molecules or OH^--ions) through the film of the corrosion products is retarded and may contribute to the process control type. If this is the case, all the three electrochemical techniques provides us with the rates of the CT process, which is not (the only) rate determining step.

3. The corrosion rates measured by the non-electrochemical techniques (gas evolution and mass loss) are more relevant to the *total* corrosion process. While these techniques cannot give us anything concerning the mechanism, they are much more accurate in the practical sense.

CONSLUSIONS

The corrosion of MRI230D magnesium alloy was measured by three electrochemical and two non-electrochemical techniques. The corrosion rates measured by different methods show large discrepancies. All the electrochemical techniques provide the corrosion rates whose values are by an order of magnitude larger than those measured by the mass loss and gas evolution.

The electrochemical techniques show that the corrosion process is complex and its rate is partially limited by the diffusion of the reducer to the metal surface. The higher values of the corrosion rate calculated from the electrochemical measurements may reflect the faster charge-transfer step rather than the r.d.s.

The non-electrochemical methods provide more realistic values of the corrosion rates while the electrochemical methods reveal the details of the process mechanism.

The PEO treatment of the alloy produces an oxide layer on the metal surface. This oxide layer is capable of some protection of the metal so that the corrosion rate for a PEO treated alloy is always lower that for the 'raw' alloy. The PEO treatment also makes the alloy a little nobler.

For both the 'raw' and the PEO treated alloy the corrosion process has a highly localized character, when 0.5-1 mm pits forms. The lifetime of an individual pit is 3-5 hours for the 'raw' and 8-10 hours for the oxidized alloy.

REFERENCES

[1]. Arrabal R., Pardo A., Merino M. C., Mohedano M., Casajús P., Paucar K. and Garcés G. (2012), “Effect of Nd on the corrosion behavior of AM50 and AZ91D magnesium alloys in 3.5 wt.% NaCl solution”, Corrosion Science Vol. 55 pp. 301–312.

[2]. Atrens A., Song G., Cao F., Shi Zh., Bowen P. (2013), “Advances in Mg corrosion and research suggestions,” J. of Magnesium and Alloys Vol.1 pp. 177-200.

[3]. Chen J., Wang J., Han E., Dong J. and Ke W. (2007), “AC impedance spectroscopy study of the corrosion behavior of an AZ91 magnesium alloy in 0.1M sodium sulfate solution”, Electrochimica Acta Vol. 52 pp. 3299–3309.

[4]. Lugovskoy A. and Zinigrad M., "Plasma Electrolytic Oxidation of Valve Metals" in "Materials

Science - Advanced Topics", Ed. Mastai Y., InTech 2013, pp. 85-102.

[5]. Qiao Z., Shi Z., Hort N., Abidin N. I. Z. and Atrens A. (2012), “Corrosion behavior of nominally high purity Mg ingot produced by permanent mold direct chill casting”, Corrosion Science. Vol. 61 pp. 185-207.

[6]. Shi Z. and Atrens A. (2011), “An innovative specimen configuration for the study of Mg corrosion”, Corrosion Science Vol. 53 pp. 226–246.

[7]. Song G., Atrens A. and Dargusch M. (1999), “Influence of microstructure on the corrosion of diecast AZ91D”, Corrosion. Science. Vol. pp. 249–273.

Notes:

1. MRI alloys, available at: http://www.dsmag.co.il/?cmd=products.5#MRI%20Alloys (accessed on 25 June 2014).